Manipulation of Interfacial Diffusion for Controlling Nanoscale Transformation

Jinxing Chen,[†,‡] *Feng Jiang,* [†,§] *Yadong Yin*[†*]

[†] Department of Chemistry, University of California, Riverside, CA 92521, USA

[‡] Institute of Functional Nano & Soft Materials (FUNSOM), Jiangsu Key Laboratory for Carbon-Based Functional Materials & Devices, Soochow University, Suzhou, Jiangsu 215123, P.R. China

[§] School of Minerals Processing and Bioengineering, Central South University, Changsha, Hunan 410083, P. R. China.

CONSPECTUS:

The unprecedented development of inorganic nanostructure synthesis has paved the way toward their broad applications in areas such as food science, agroforestry, energy conversion, and biomedicine. The precise manipulation of the nucleation and subsequent growth has been recognized as the central guiding principle for controlling the size and morphology of the nanostructures. However, conventional colloid syntheses based on direct precipitation reactions still have limitations in their versatility and extendibility. The crystal structure of a material determines the limited number of possible morphologies that its nanostructures can adopt. Further, as nucleation and growth kinetics are sensitive to not only the nature of the precipitation reactions but also ligands and ripening effect, rigorous control of reaction conditions must be established for every specific synthesis. In addition, multiple experimental parameters are entangled with each

other, thereby requiring rigorous control of all reaction conditions. As a result, it is usually challenging to extend a synthetic recipe from one material to another. As an alternative method, the direct transformation of existing nanostructures into target ones has become an effective and robust approach capable of creating various complex nanostructures that are otherwise challenging to obtain using conventional methods. To this end, an in-depth understanding of nanoscale transformation toward the synthesis of inorganic nanostructures with diverse properties and applications is highly desirable.

In this Account, we aim to reveal the critical effect of the interfacial diffusion on controlled nanoscale transformation. We first discuss how the interdiffusion rates determine the morphology and property of bimetallic nanostructures. While equal interdiffusion rates lead to perfect mixing and generate fully alloyed nanostructures, interdiffusion at unequal rates creates vacancies in the fast diffusion side, which may cause the dramatic morphological transformation to the nanostructures. Then, we introduce interfacial reactions, including the Kirkendall cavitation process, elimination reaction, and solid-state reaction, to promote the unbalanced interdiffusion and generalize nanoscale transformations in materials of various compositions, morphologies, and crystal structures. Finally, we discuss the use of capping ligands to inhibit the diffusion of atoms on one side of the interface in order to enable selective etching or transformation of the nanostructures. By modifying the nanostructured surface with specific capping ligands, the diffusion of surface atoms is restricted. When nanoparticles undergo chemical reactions (such as etching or heating), the outward diffusion of substances dominates, thereby successfully achieving chemical and morphological transformations. We believe that controlled interfacial diffusion can effectively manipulate nanoscale transformations, thus providing new strategies for the custom synthesis of multifunctional nanomaterials for various specific applications.

KEY REFERENCES

- Gao, C.; Hu, Y.; Wang, M.; Chi, M.; Yin, Y. Fully alloyed Ag/Au nanospheres: combining the plasmonic property of Ag with the stability of Au. *J. Am. Chem. Soc.* **2014**, *136*, 7474−7479.[1] By heating *Au@Ag nanospheres near to their melting points,* homogeneous *Ag/Au alloy nanospheres can be obtained, which combine the high plasmonic activity of Ag and remarkable stability of Au.*

- Yin, Y.; Rioux, R.; Erdonmez, C.; Hughes, S.; Somorjai, G; Alivisatos P. Formation of hollow nanocrystals through the nanoscale Kirkendall effect. *Science*, **2004**, *304*, 711-714.[2] *The nanoscale Kirkendall effect was used to produce hollow nanostructures for the first time by taking advantage of the dominant outward diffusion of core materials driven by chemical transformations.*

- Tianou, H.; Wang, W.; Yang, X.; Cao, Z.; Kuang, Q.; Wang, Z.; Shan, Z.; Jin. M.; Yin, Y. Inflating hollow nanocrystals through a repeated Kirkendall cavitation process. *Nat. Commun.* **2017**, *8*, 1261.[3] *Dominant outward diffusion of core species can be driven by an elimination reaction and produce Kirkendall voids in metal nanocrystals. By repeating the Kirkendall cavitation process, the hollow metal nanocrystals have ultrathin shells.*

- Wu, L.; Hu, H.; Xu, Y.; Jiang, S.; Chen, M.; Zhong, Q.; Yang, D.; Liu, Q.; Zhao, Y.; Sun, B.; Zhang, Q.; Yin, Y. From nonluminescent Cs_4PbX_6 (X = Cl, Br, I) nanocrystals to highly luminescent $CsPbX_3$ nanocrystals: water-triggered transformation through a CsX-stripping mechanism. *Nano Lett.* **2017**, *17*, 5799−5804.[4] *An elimination reaction can strip CsX (X =*

Cl, Br, I) from nonluminescent Cs_4PbX_6 nanocrystals and enable their efficient chemical transformation to highly luminescent $CsPbX_3$ nanocrystals.

INTRODUCTION

The controllable synthesis of nanostructured inorganic materials has remained the focus of materials research because they may offer many intriguing new properties that can be achieved by tailoring their compositions and structures.[5-12] Although significant progress has been made in producing various nanostructures through conventional synthesis approaches, it is still challenging to rationally design the desired structures in a highly predictive manner. Besides, the effects of experimental parameters in conventional synthesis are often entangled, thereby demanding rigorous control of reaction conditions.[13,14] Methods based on transforming existing nanostructures into target ones may allow straightforward prediction of products and independent control over reaction parameters.[15-17] Such chemical transformation processes are emerging as new platforms for the design and synthesis of next-generation nanocrystals, which have been difficult to prepare by conventional approaches.

In a recent example, Schaak et al. have provided two design guidelines for synthesizing a heterostructured nanorod library.[15] By performing seven sequential cation exchange reactions on the precursor of copper sulfide nanorods, a feasible route for the synthesis of 65,520 unique multicomponent metal sulfide nanorods was determined, and 113 individual heterostructured nanorods were experimentally proved. Such versatility and extendability are rarely found in conventional colloid syntheses. As another example, we have developed a thermal dewetting strategy that can be carried out in confined spaces for fabricating Au nanocups with a controllable opening size and a hollow interior, which are thermodynamically unfavored and therefore difficult

to produce by conventional colloidal synthesis methods.[18] In this case, the morphology of the Au nanocups is determined solely by the pre-designed nanospace, thus ensuring high process reproducibility and high product uniformity. Also, chemical transformation strategies may offer opportunities to fine-tune the morphologies of the nanostructures originally favored under special kinetic control so that they become more suitable for the target applications. A good example is the transformation of Ag nanoplates from triangular to more stable circular shape by light-induced surface diffusion.[19]

The chemical transformation of inorganic nanostructures is typically driven by their interactions with the surroundings, therefore involving diffusion of atoms across various surfaces and interfaces.[20] Comprehensive understandings of interfacial diffusion are therefore vital and necessary for improving our capability in controlling the nanoscale transformation processes. While its importance has been noted in some articles, unfortunately, interfacial diffusion has rarely been discussed in detail in the context of chemical transformation. Herein we aim to discuss our understanding of the effect of interfacial diffusion on nanoscale transformation based on the relevant results obtained in our research. We first use the bimetallic nanostructures as examples to introduce the concept of nanoscale interfacial diffusion because of not only the relative simplicity of the diffusion couples but also the strong impact of the diffusion processes on their unique optical and catalytic properties. In these cases, interfacial diffusion is a passive behavior that relies on temperature rise to promote the thermal migration of atoms. Further, we discuss the active manipulation of interfacial diffusion by introducing chemical reactions, which induce substantial structural transformation that leads to dramatic morphological changes. Our discussions will include the cavitation process induced by the nanoscale Kirkendall effect, the interfacial solid-state reaction, the interfacial stripping or dissolution process, and the surface-protected etching

process. Finally, we summarize the current progress and provide some personal views of future research development in the related fields.

2. MANIPULATION OF INTERFACIAL DIFFUSION

2.1 Interfacial diffusion in bimetallic nanostructures

The interdiffusion of atoms between two metals was historically the focus of the study that led to the discovery of the fundamental mechanism of atomic migration.[21] Recently, bi- and multi-metallic nanostructures were found to play important roles in catalysis, plasmonics, and biomedicine,[22,23] as interfacial diffusion in multi-metallic nanostructures may cause significant modifications to the composition of the surface and the bulk of the nanoparticles, thereby dramatically change their properties. Fine-tuning the interfacial diffusion can thus offer great opportunities to optimize their structures to meet the requirements of various applications.[22] As schematically shown in Figure 1a, the interdiffusion of metals A and B with equal rates is expected to lead to uniform mixing of atoms, eventually forming an alloy or intermetallic nanostructure. However, it is rare for two metals to have the same diffusion coefficient in each other. According to Fick's first law of diffusion, when a diffusion couple of two metals is heated to temperatures that atomic diffusion becomes pronounced, the flux of atoms from the metal with the higher diffusion coefficient is larger than the opposite one, and the net flux of atoms from the metal with the higher diffusion coefficient into the one with the lower diffusion coefficient has to be balanced by a flux of vacancies in the opposite direction. These vacancies may be annealed out of the metal to result in an overall shift of the interface toward the metal with the higher diffusion coefficient or accumulate and then coalesce into voids that can grow from nanoscale to micro and macroscale

upon continuous interdiffusion.[24] The interdiffusion process described above is recognized as the Kirkendall effect,[15,21] and the resulting voids are often referred to as the Kirkendall voids.

While the Kirkendall effect was originally observed in bulk samples, it can also occur in nanoscale objects. However, different from the bulk phase, the vacancies created in a nanoscale diffusion couple can be easily eliminated by migrating to the surface and inducing surface reconstruction, making it challenging to maintain a high vacancy concentration. Typically, thermally driven diffusion can only create a low concentration of vacancies, which are difficult nucleate and grow into voids or can only grow into small voids in nanostructures. Nevertheless, we have observed the void formation resulting from interfacial diffusion in the Pd@Au bimetallic core-shell nanocubes (Figure 1b-1c).[25] Onto pre-synthesized Pd nanocubes, a layer of Au was deposited by slow injection of triphenylphosphinegold(I) chloride ($AuPPh_3Cl$), followed by reduction by oleylamine. Using the Au(I) precursor instead of the typical Au(III) precursor minimizes the galvanic replacement reaction. Since Pd and Au are miscible in all proportions with only a small lattice mismatch (4.9%), the deposition leads to the conformal coating of Au and produces Pd@Au core-shell nanocubes. By heating the colloidal dispersion at 200 °C, substantial interdiffusion of the atoms was initiated at the interface, resulting in the formation of Au-Pd alloy on the surface and some Kirkendall voids. As shown in Figure 1c, the Pd core within the alloy shell and the voids within each Pd core could be well-resolved thanks to the high contrast between Pd and Au-Pd alloy in the high-angle annular dark-field scanning transmission electron microscopy (HAADF-STEM). The relatively low concentration of vacancies could only support the formation of one or two small voids in each nanocube. In addition to temperature, the dimension of the diffusion couple becomes an important factor in determining the extent of interdiffusion and, subsequently, the amount and concentration of vacancies that can be produced

in nanoscale objects. As revealed in a separate study involving heating Pd@Au core-shell nanostructures with a thin Au shell, the interdiffusion was substantially limited so that no voids could be observed due to the low vacancy concentration.[26]

The interfacial diffusion of core-shell bimetallic nanostructures can effectively modify the core metal surfaces with the shell atoms without significantly altering the crystal facets on the original core surface. Such modification provides opportunities to effectively tune the electronic structure of the catalysts to boost their catalytic activity. As demonstrated in Pd@Au nanocubes, the optimized surface alloy catalyst demonstrates the greatly enhanced activity and selectivity toward alkyne semihydrogenation reactions than commercial Pd/C and Lindlar catalyst.[25] The same interfacial diffusion strategy can be extended to produce other Pd-M (M = Ni, Ag, Cu) alloy surfaces on Pd nanocubes to significantly improve the selectivity in the hydrogenation of chloronitrobenzenes, with Pd-Ni alloy surface reaching the highest catalytic selectivity (> 99%).[27]

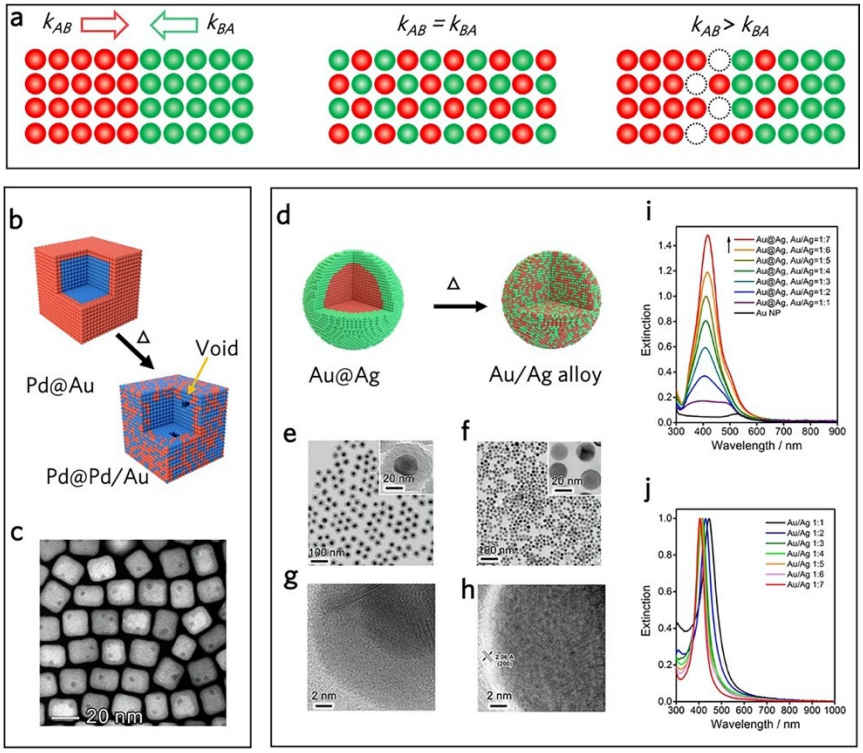

Figure 1. Interfacial diffusion in the bimetallic system. a, Schematic of typical interfacial diffusion with different interdiffusion rates. **b,** Schematic of interfacial diffusion of Pd@Au nanocubes. **c,** HAADF-STEM image of Pd@Au-Pd alloy surface nanocubes with several holes on the Pd side. Reproduced with permission from Ref. 25. Copyright 2017, The Royal Society of Chemistry. **d,** Schematic illustration of alloy process of Au@Ag core-shell nanoparticles. **e, f,** TEM images of Au@Ag@SiO_2 (e) and Au/Ag alloy (f) nanoparticles. **g, h,** HRTEM images of Au@Ag (g) and Au/Ag alloy (h) nanoparticle. **i, j,** UV−vis extinction spectra of Au@Ag core-shell (i) and Ag/Au alloy (j) nanoparticles with different Ag/Au ratios. Reproduced with permission from Ref. 1. Copyright 2014, American Chemical Society.

At the nanoscale, extensive interdiffusion of two miscible metals eventually leads to the formation of alloy nanostructures, which often exhibit beneficial properties that a single metal does not possess. A good example is the case of Ag and Au. Ag exhibits the strongest surface plasmon resonance than other metals, but the applications of its nanostructures are limited by poor chemical stability. On the contrary, Au is considered chemically stable, but it is more expensive and possesses much weaker plasmonic activity than Ag. Forming Ag/Au alloy is therefore desirable to produce new plasmonic nanostructures that combine the advantages of the two and avoid their disadvantages. While simple co-reduction approaches have been explored,[28-34] the compositional and structural homogeneity has been lacking due to the different reduction kinetics of the two metal precursors, which result in stepwise reduction and growth.[35] To this end, we have developed a surface-protected annealing process to enable full interdiffusion of Ag and Au into one another while preventing the interparticle coalescence (Figure 1d).[1,36] The interfacial diffusion occurs in Au@Ag core/shell nanoparticles when they are annealed at ∼1000 °C under an inert atmosphere, which is close to their melting points (1064.2 °C for bulk Au and 961.8 °C for Ag). A silica layer

was pre-coated on the Au@Ag nanoparticles through a sol-gel method to prevent nanoparticles from aggregation during the high-temperature treatment (Figure 1e-1f). The extensive atomic interdiffusion contributes to removing crystallographic defects and, more importantly, the elimination of compositional interfaces (Figure 1g-1h), therefore providing the alloy nanoparticles an extremely narrow and sharp plasmonic resonance peak (Figure 1i-1j). The same strategy could be extended to the generation of anisotropic Ag/Au alloy nanorods.[37] The resonant frequency and peak intensity of both transverse and longitudinal modes of the alloyed products could be well-tuned. With their high stability against chemical etching and high plasmonic activity, such alloy nanostructures are expected to significantly broaden the applications of plasmonic nanostructures, especially in areas involving corrosive species.

2.2 Nanoscale transformation driven by interfacial reactions

2.2.1 Kirkendall cavitation process

Thermally driven interdiffusion often does not cause a substantial transformation of nanostructures at relatively low temperatures due to the generation of a low concentration of vacancies. A chemical reaction may provide a much higher driving force to promote the interdiffusion of atoms. In particular, in the case of colloidal nanoparticles reacting with chemicals dissolved in solution, there naturally exists a high concentration contrast between the solid core and dispersed reactants, which inherently favors the outward diffusion of the core species. A significantly faster outward diffusion than the inward diffusion of atoms will be balanced by the injection of vacancies to the core, which will then nucleate into voids at the boundary of the original core and the resulting shell. The continued chemical reaction supports the further growth

of the voids and promotes their eventual coalescence into a single large void within the nanoparticle.

Such a significant transformation was observed in the Ag/Au bimetallic nanoparticle system, where the interdiffusion was driven by the galvanic replacement of Ag atoms on Ag nanocrystals by Au(III) species dissolved in a solution.[38] Due to the higher reduction potential of $AuCl_4^-$/Au (0.99 V *vs.* standard hydrogen electrode (SHE)) than Ag^+/Ag (0.80 V *vs.* SHE), Au(III) species were reduced into Au(0) and deposited on the surface of Ag cores to produce an Ag/Au shell, while the surface Ag atoms were oxidized and dissolved in solution.[39] Further reaction required the diffusion of core Ag atoms to the surface, promoting the formation of vacancies within the nanocrystal. As shown in Figure 2a-2b, hollow nanocrystals of Ag/Au alloy were eventually obtained when the vacancies have coalesced into a single void. Besides the high concentration difference of Au and Ag atoms across the shell, the outward diffusion of Ag was also favored by its higher diffusion rate than Au in the bimetallic diffusion couple.[40] In addition, the stoichiometry of this galvanic replacement is also believed to contribute to the preferential outward diffusion of the Ag atoms, as the deposition of every Au atom would ideally release three Ag atoms from the nanocrystal, while the atomic radii of the two metals are very similar. It is also interesting to point out that the deposition of Au atoms occurred preferentially onto the high energy (100) and (110) facets of the nanocrystals, turning the single-crystalline Ag nanospheres into hollow Ag/Au alloy nanocrystals with a truncated octahedral shape enclosed by six (100) and eight (111) facets.

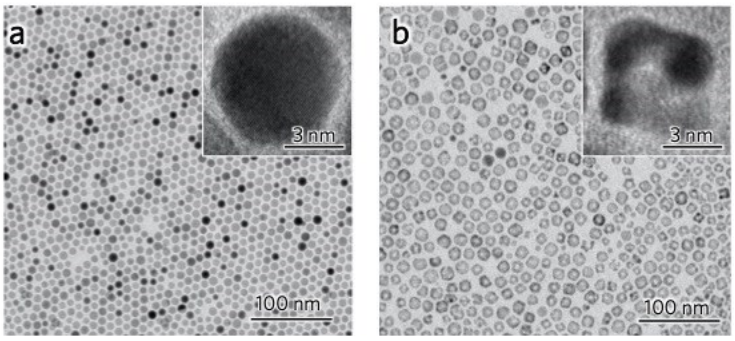

Figure 2. Nanoscale transformation by galvanic replacement reaction. a, b, TEM images of Ag nanocrystals (a) and hollow Au nanocrystals obtained by performing a replacement reaction on the Ag nanocrystals in the image (a). Insets are the corresponding HRTEM images of an Ag and an Au hollow nanocrystal. Reproduced with permission from Ref. 39. Copyright 2006 American Chemical Society.

The contribution of interdiffusion along with the galvanic replacement to the void formation has been confirmed by a number of groups. For example, Puntes et al. prepared Au-Ag alloy/Ag/Au-Ag alloy trilayered nanoboxes and reacted them with Au(I) species, which has a lower reduction potential than Au(III) and therefore decreased replacement kinetics.[41] As the replacement reaction consumed the Ag atoms in the alloyed shells, it increased the concentration gradient of Ag atoms from the sandwiched Ag layer to the alloyed surface and promoted the outward diffusion of Ag atoms, eventually hollowing out the Ag layer and forming double-walled nanoboxes. Mirsaidov et al. studied the transient stages of the galvanic replacement reaction between Ag nanocubes and Au(III) using liquid cell TEM and confirmed that hollowing was achieved via nucleation and growth and coalescence of voids inside the nanocubes.[42]

The reaction-driven nanoscale transformation based on the Kirkendall effect is not limited to metallic nanostructures but also applies to those with more complex compositions. For example, in 2004, we first introduced the nanoscale Kirkendall effect to prepare hollow cobalt chalcogenide

nanocrystals.[2] Specifically, metallic cobalt nanocrystals were reacted with elemental sulfur or selenium in o-dichlorobenzene at 180 °C to produce cobalt chalcogenide hollow nanocrystals. A single void was formed in each nanocrystal due to the much faster outward diffusion of cobalt than the inward diffusion of sulfur or selenium. The transformation process was studied by monitoring the reaction of cobalt nanocrystals with selenium. As shown in Figure 3, a thin cobalt selenide shell formed on the surface of the cobalt nanoparticle after a short period of reaction (10 s). Between the core and the shell, a thin gap was found to form due to vacancy coalescence. Thin filaments were found to connect the core and shell to allow the continued outward diffusion of cobalt atoms. As the reaction proceeded further, the core and the filaments shrank and eventually disappeared, producing well-defined hollow nanocrystals. As expected, the same mechanism could be applied to nanostructures of other shapes, such as cobalt nanodisks. It was also found that increasing reaction temperature made the diffusion of vacancy more favorable, promoting the formation of a uniform hollow structure with a single circular void located in the center.[43]

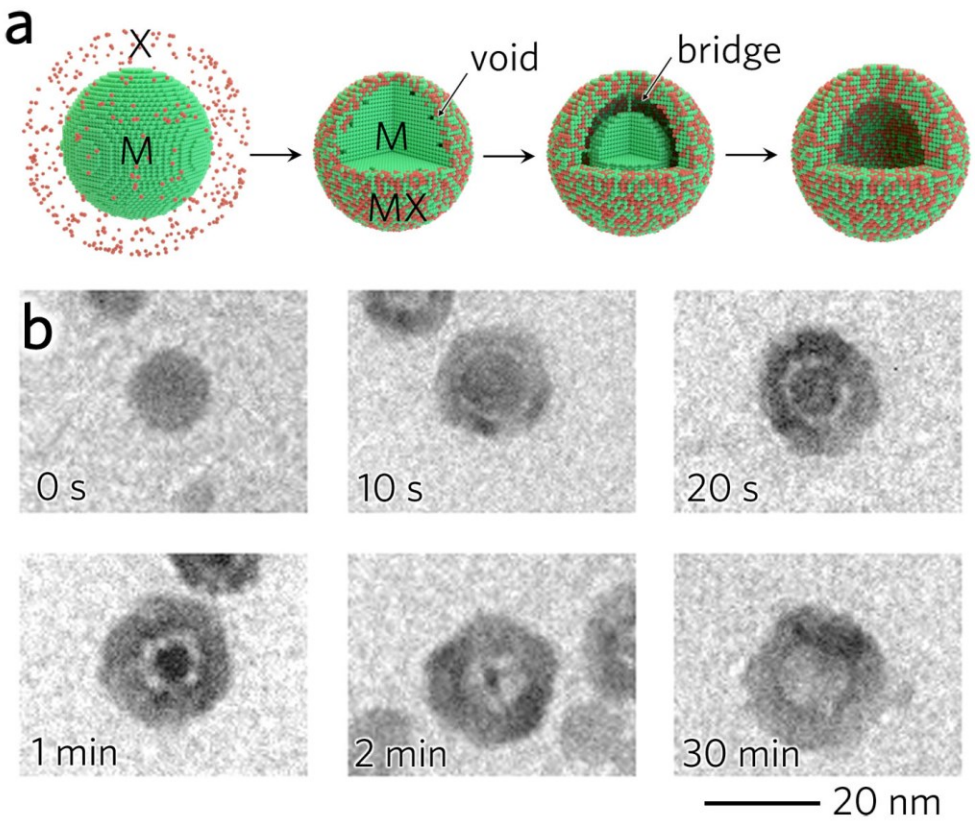

Figure 3. Nanoscale Kirkendall cavitation process. a, Schematic illustration of the nanoscale Kirkendall cavitation process. **b,** Hollowing process of CoSe nanocrystals by injection of a suspension of selenium/o-dichlorobenzene into a cobalt nanocrystal solution at 455 K. Reproduced with permission from Ref. 2. Copyright 2004, the American Association for the Advancement of Science.

In general, when a nanocrystal M reacts with a chemical species X to produce MX, the Kirkendall voids form only when the outward diffusion of M is faster than the inward diffusion of X. When the inward diffusion of X is faster, the final product of MX is expected to be solid nanocrystals. However, if X can be extracted from the MX nanocrystals, the outward diffusion of X may still be faster than the inward diffusion of M, so vacancies can be injected into the core, again resulting in Kirkendall voids.[3] The challenge is finding the appropriate extraction reaction

to enable the preferential outward diffusion of X. Recently we have demonstrated such a process by extracting P from PdP_2 nanocrystals, which were produced by reacting Pd nanocubes with trioctylphosphine (TOP) at 250 °C (Figure 4a). The extraction reaction was conducted by oxidizing PdP_2 nanocrystals (Figure 4b) using air in oleylamine at 250 °C, generating hollow Pd nanocrystals (Figure 4c). The key of this structural transformation is the much faster outward diffusion of P than Pd atoms, which benefits from the strongly favored reaction of P with O_2. Therefore, by controlling the O_2 concentration in the system, it is convenient to tune the diffusion rate of P and manipulate the overall morphology of the resulting nanocrystals. Additionally, the reaction temperature also determines the nanostructure transformation process in vacancy creation and void coalescence. Below 150 °C, the extraction process only led to porous Pd nanocrystals instead of hollow ones.

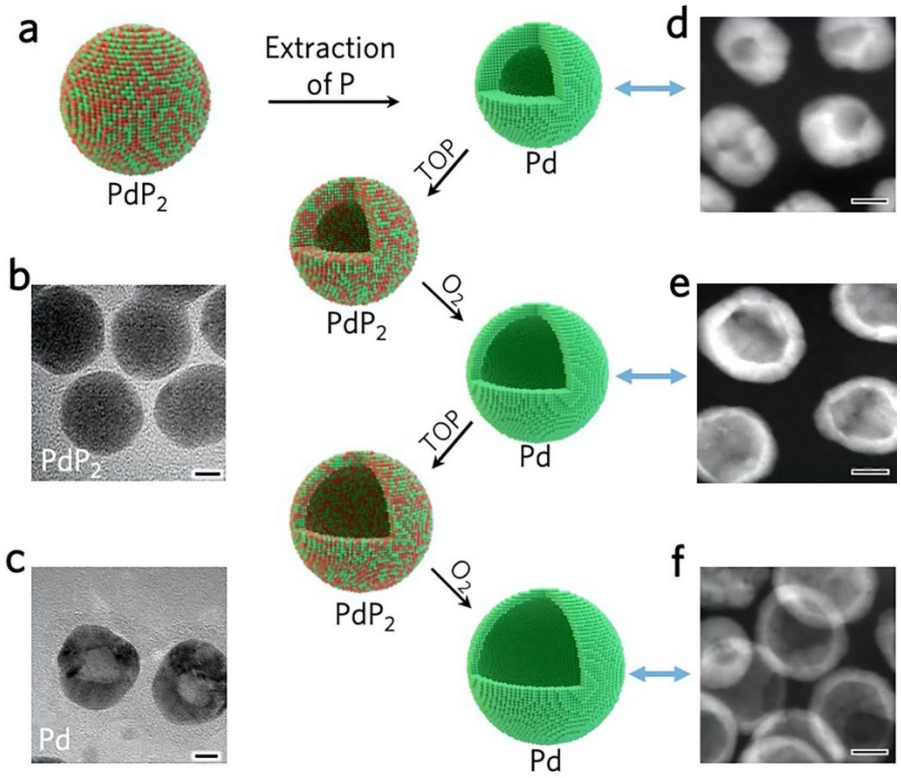

Figure 4. Formation of hollow nanocrystals through a repeated Kirkendall cavitation process. a, Schematic illustration of the synthetic strategy of hollow metal nanocrystals. **b, c,** TEM images of PdP_2 intermediates, and hollow Pd nanospheres. **d-f,** HAADF-STEM images of the hollow Pd nanocrystals after one (d), two (e), and three (f) cavitation cycles. All scale bars are 5 nm. Reproduced with permission from Ref. 3. Copyright 2017, Springer Nature Publishing Group.

An interesting feature of this reaction is that the addition and extraction of P can be repeated, allowing the gradual enlargement of the Kirkendall voids and thinning of the shells. As shown in Figure 4d, the first cycle resulted in hollow Pd nanocrystals with a diameter of ~20.7 nm and a void size of ~7.5 nm. After reacting with TOP, the Pd nanocrystals were converted back to PdP_2 while retaining the hollow structure. The subsequent extraction process further enlarged the shells to a diameter of 25.3 nm and void size of 16 nm, yielding thinner shells (Figure 4e). Further repeating the cycle produced Pd nanocrystals with an outer diameter of 26.4 nm and pore size of 19.2 nm (Figure 4f). The shell thickness decreased as thin as 2-3 nm, which is of great interest for catalytic applications.

2.2.3 Elimination reaction

Various types of chemical reactions can be used to initiate transformations of nanostructures. Recently, we have revealed that the transformation of perovskite nanocrystals through an elimination reaction at liquid interfaces.[4,44-47] As shown in Figure 5a, non-luminescent Cs_4PbX_6 (X = Cl, Br, I) nanocrystals dispersed in hexane can be converted to highly luminescent $CsPbX_3$ nanocrystals by stripping CsX through an interfacial reaction with water. At the hexane/water interface, the Cs_4PbX_6 nanocrystals converted into $CsPbX_3$ phase by eliminating CsX from their crystal lattice. Driven by the high solubility of CsX, the elimination reaction was associated with

the lattice reconstruction, which led to changes in nanocrystal morphology. As shown in an example in Figure 5b-5c, spherical Cs_4PbBr_6 nanocrystals with a diameter of ~17.8 nm were transformed into cubelike structures of $CsPbBr_3$ with an edge length of ~12.2 nm. In addition, the products dissolved in the water phase were found to be mostly CsX, which is consistent with our proposed mechanism. Accordingly, under UV excitation, green luminescence of $CsPbBr_3$ was initially observed only at the hexane/water interface, but later in the entire hexane phase on the top, proving the successful structural transformation of all nanocrystals (Figure 5d). With this strategy, $CsPbX_3$ nanocrystals with various halide compositions could be obtained by transforming their corresponding Cs_4PbX_6 precursor nanocrystals. Thanks to their strong composition-dependent luminescence properties, the luminescence of the resulting nanocrystals could cover the full visible range (Figure 5e).

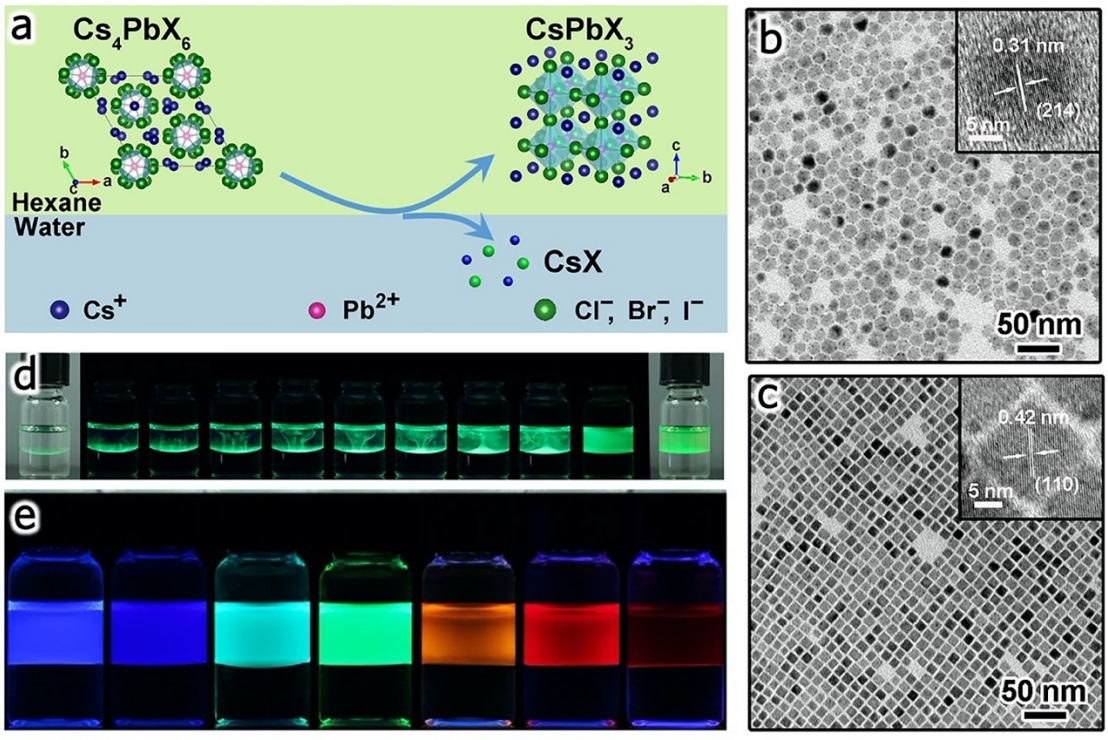

Figure 5. The water-triggered transformation from Cs_4PbX_6 (X = Cl, Br, I) nanocrystals to $CsPbX_3$ nanocrystals. **a,** The transformation process of Cs_4PbX_6 to $CsPbX_3$ by water treatment.

b, c, Representative TEM images of Cs_4PbBr_6 (b) and $CsPbBr_3$ (c) nanocrystals. **d,** The samples were illuminated with UV light (λ = 365 nm) with different transformation times. **e,** Photographs of $CsPbX_3$ nanocrystals dispersed in hexane under UV light (λ = 365 nm) illumination. From left to right, the nanocrystals are obtained using Cs_4PbCl_6, $Cs_4PbCl_{4.5}Br_{1.5}$, $Cs_4PbCl_3Br_3$, $Cs_4PbBr_{4.5}I_{1.5}$, $Cs_4PbBr_3I_3$, and Cs_4PbI_6 nanocrystals as the precursors. Reproduced with permission from Ref. 4. Copyright 2018, American Chemical Society.

2.2.4 Solid-state reaction

Besides colloidal systems, nanoscale transformation can also be achieved by interfacial reactions at the solid-state. Figure 6a shows the transformation of Fe_3O_4 nanoparticles by reacting with the encapsulating SiO_2.[48] When the Fe_3O_4@SiO_2 core-shell nanoparticles (Figure 6b) were heated in hydrogen gas at 500 °C for 4 h, the Fe_3O_4 cores were reduced to FeO, which would further react with SiO_2 to form Fe_2SiO_4. The dissolution of Fe_2SiO_4 in the SiO_2 shell drove the outward diffusion of iron oxide species and, accordingly, the inward diffusion of vacancies, which coalesce into voids. If the number of iron species exceeded its solubility in the silica shell, a FeO core of reduced size would remain inside the shell, as shown in Figure 6c. Upon switching the atmosphere from hydrogen to air and heating for another 4 h, the iron species were oxidized back to Fe_3O_4, which precipitated from the shell due to its low solubility in SiO_2. As the inward diffusion and nucleation of Fe_3O_4 was energetically unfavored, Fe_3O_4 migrate preferentially outward, forming a new particle attached to the outer surface of each shell (Figure 6d).

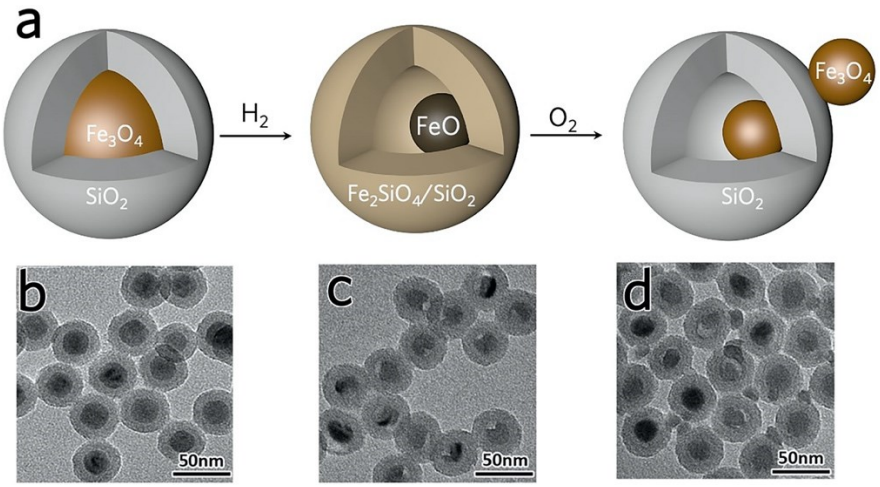

Figure 6. Solid-state transformation of iron oxide nanoparticles by the redox-buffering effect. **a,** Schematic shows the solid-state transformation of iron oxide nanoparticles through a silica shell. **b-d,** TEM images of original iron oxide@silica core−shell nanoparticles (a) after being treated with H_2 at 500 °C for 4 h (b) and then with air at the same temperature for another 4 h (c). Reproduced with permission from Ref. 48. Copyright 2018, American Chemical Society.

2.3 Nanoscale transformation through surface passivation

In the above systems, our focus has been primarily on enhancing the diffusion ability of one species to achieve a difference in interfacial diffusion. We have also explored approaches to increase the contrast in diffusion rate by suppressing the diffusion of a particular species, for example, by binding the nanostructured surface with specific capping ligands. With sufficient surface protection, the surface structure can be greatly stabilized, while the species inside may be selectively removed and diffuse out, producing a hollow nanostructure.

The surface-passivated nanoscale transformation involves surface modification of a pre-synthesized nanostructure with a layer of polymeric ligands, followed by heat treatments or selective etching to promote the outward diffusion of materials from the core (Figure 7a).[49] This strategy was initially demonstrated in the conversion of solid TiO_2 microspheres to hollow

nanocapsules,[50] where amorphous TiO_2 microspheres were protected by surface-bound poly(acrylic acid) (PAA) and then etched by diethylene glycol (DEG) at 200 °C. In this case, PAA plays a vital role by "crosslinking" the TiO_2 grains on the surface, allowing only the inner part to be selectively dissolved by DEG. The concept was later extended to the synthesis of SiO_2 hollow spheres. Poly(vinyl pyrrolidone) (PVP) was used as the capping ligand because of its strong hydrogen bonds with the hydroxyls on silica surface. With the establishment of a considerable contrast in stability against the etching by OH^- between the surface and interior of the SiO_2 spheres, the core can be selectively removed, generating hollow structures.[51,52] Notably, the overall size of the SiO_2 remained unchanged upon etching, proving sufficient surface passivation (Figure 7b). Since many nanoparticles can be embedded in SiO_2 through colloidal coating, this strategy is particularly useful for encapsulating functional nanostructures in porous SiO_2 nanoshells to produce highly stable nanoscale reactors for sensing and catalytic applications.

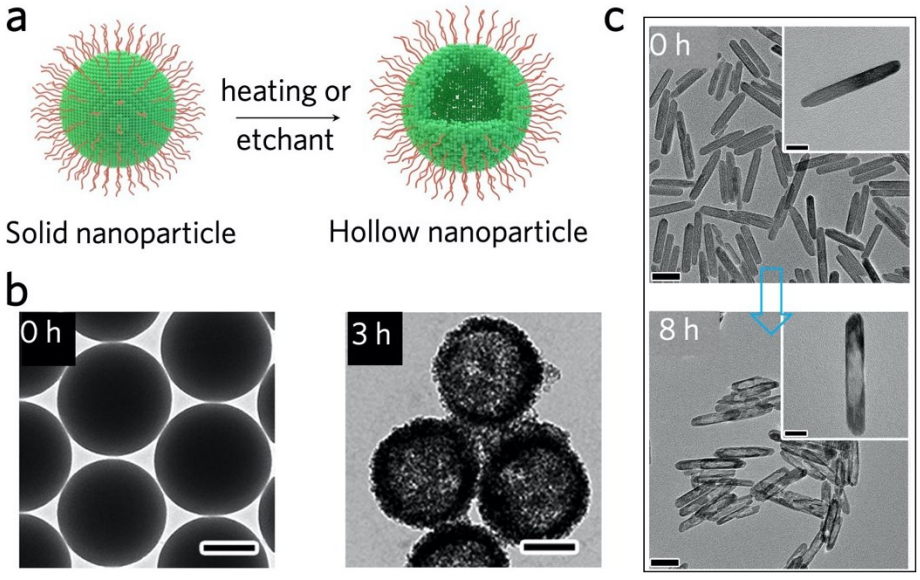

Figure 7. Nanoscale transformation through surface-passivation. a, Schematic illustration of the concept of surface-passivation etching. **b,** TEM images of PVP-treated SiO_2 particles before and after etching by NaOH for 3 h. Scale bars are both 200 nm. Reproduced with permission from

Ref. 51. Copyright 2007, American Chemical Society. **c.** TEM images of β-FeOOH nanorods before and after transformation. Scale bars are 50 nm, and insets are 20 nm. Reproduced with permission from Ref. 53. Copyright 2017 American Chemical Society.

Although the surface-passivation strategy was initially proposed for selective etching, our recent results show that it can be greatly generalized to the chemical transformation of nanocrystals,[53-55] making it particularly useful for synthesizing nanocrystals that are difficult to obtain conventional approaches. For example, with the protection of PAA, the solid β-FeOOH nanorods could be transformed into hollow Fe_3O_4 counterparts by DEG reduction at 220 °C while retaining the rod shape (Figure 7c). We have further demonstrated the generality of this approach by chemically transforming other nanomaterials and morphologies, such as α-Fe_2O_3 spherical nanoclusters, $Co(OH)_2$ nanoplates, and Prussian blue nanocubes.

Although it is generally believed that the surface-passivated conversion achieved by capping ligands is useful in solution phase reaction, we have demonstrated their presence in solid-state calcination not only preserved the overall morphology but also effectively created controllable pores in metal oxide nanostructures.[56,57] We used the chemical conversion of β-FeOOH nanostructures into α-Fe_2O_3 and magnetic Fe_3O_4 phases as an example and found that polymeric ligands could protect the surface atoms from diffusion during the solid-state transformation. The strong coordinating interaction between the capping ligands and nanostructure surface made it possible for the morphological preservation and additional prevention of the fusion of internal grains. This finding refines our understanding of the protection function of capping ligands to nanostructures and expands their effectiveness from conventional solution-phase reaction to high-temperature solid-state transformation.

3. CONCLUSIONS AND PERSPECTIVES

Interfacial diffusion is the cause of many interesting phenomena relevant to inorganic nanostructures. It can also be utilized as a new platform for the design and synthesis of nanostructures that are difficult to prepare using conventional approaches. By controlling the interdiffusion rates at the interface, it is possible to achieve fully alloying of the two metals or to generate complex nanostructures with defects and porosity on the one side of the diffusion couple. Many more opportunities can be expected when the concept is extended to controlling the interdiffusion of multi-metallic nanostructures, although it would be challenging to analyze such systems as many components and interfaces are involved. For example, controlling the interdiffusion over multi-metallic components within one particle may lead to the formation of high-entropy alloys, which are believed to have significant impacts on nanocatalysis and structural engineering.

Chemical reactions can often provide a more significant driving force than thermal-driven processes for promoting interfacial diffusion, therefore offering more opportunities to initiate a substantial nanoscale transformation. As a classic phenomenon in metallurgy, the Kirkendall effect has now become a unique strategy to transform solid nanocrystals into various hollow structures by taking advantage of the different diffusion rates of species involved in the chemical reactions of nanoscale objects. Though notable achievements have been made in this field, it would be interesting to explore other types of reactions rather than colloidal reactions to drive the unbalanced interfacial diffusion for creating the Kirkendall voids. More importantly, the reaction-driven interfacial diffusion may be integrated into the electrochemical, photochemical, and high-temperature calcination processes to control the morphology and structure of nanoscale materials toward the specific applications.

Surface passivation with capping ligands provides ample opportunities for shape-conserved chemical transformation, especially when combined with selective etching or phase conversion processes. The surface-passivated etching shows particular advantages for fabricating yolk-shell or rattle-type nanostructures with active nanomaterials encapsulated inside. The new surface-protected phase conversion strategy gives rise to a well-maintained morphology of the crystalline nanostructures. Considering its simplicity, the effectiveness of this strategy should be examined in many other chemical reactions in addition to the proven reduction reaction. Further, since a wide range of colloidal nanoparticles are now readily available, it will be of practical significance to explore their chemical conversion into other nanostructures with unconventional chemical and morphological features under the surface-passivated scheme.

AUTHOR INFORMATION

Corresponding Author

*Yadong Yin, yadong.yin@ucr.edu

Author Contributions

The manuscript was written through the contributions of all authors. All authors have given approval to the final version of the manuscript.

Notes

Any additional relevant notes should be placed here.

Biography

Jinxing Chen is currently a postdoctoral researcher at the University of California Riverside. He received his B.S. (2013) in polymer materials and engineering from the University of Jinan and Ph.D. (2018) in chemistry from the University of Science and Technology of China. He is interested in the synthesis of nanostructured materials for optical, energy, and environmental applications.

Feng Jiang is currently a visiting Ph.D. student at the University of California Riverside. He obtained his B.S. (2011) and M.S. (2014) in mineral engineering from Central South University in China. His research interests include the solid-state transformation of nanostructures and the functionalization of mineral materials for electrochemical energy storage.

Yadong Yin received his B.S. and M.S. in chemistry from the University of Science and Technology of China in 1996 and 1998, respectively, and Ph.D. in materials science and engineering from the University of Washington in 2002 under the supervision of Prof. Younan Xia. After working as a postdoctoral fellow at the University of California, Berkeley, and the Lawrence Berkeley National Laboratory under the supervision of Prof. A. Paul Alivisatos, he became a staff scientist at LBNL in 2005. In 2006 he joined the faculty at the Department of Chemistry, University of California Riverside. His research interests include the synthesis and application of nanostructured materials, self-assembly processes, and colloidal and interface chemistry.

ACKNOWLEDGMENT

Y.Y. is grateful for the financial support from the U.S. National Science Foundation (CHE-1808788). J.C. acknowledges the support by the National Natural Science Foundation of China (51901147) and the China Postdoctoral Science Foundation (2019M651939).

REFERENCES

(1) Gao, C.; Hu, Y.; Wang, M.; Chi, M.; Yin, Y. Fully Alloyed Ag/Au Nanospheres: Combining the Plasmonic Property of Ag with the Stability of Au. *J. Am. Chem. Soc.* **2014**, *136*, 7474-7479.

(2) Yin, Y.; Rioux, R. M.; Erdonmez, C. K.; Hughes, S.; Somorjai, G. A.; Alivisatos, A. P. Formation of Hollow Nanocrystals through the Nanoscale Kirkendall Effect. *Science* **2004**, *304*, 711-714.

(3) Tianou, H.; Wang, W.; Yang, X.; Cao, Z.; Kuang, Q.; Wang, Z.; Shan, Z.; Jin, M.; Yin, Y. Inflating Hollow Nanocrystals through a Repeated Kirkendall Cavitation Process. *Nat. Commun.* **2017**, *8*, 1261.

(4) Wu, L.; Hu, H.; Xu, Y.; Jiang, S.; Chen, M.; Zhong, Q.; Yang, D.; Liu, Q.; Zhao, Y.; Sun, B.; Zhang, Q.; Yin, Y. From Nonluminescent Cs4pbx6 (X = Cl, Br, I) Nanocrystals to Highly Luminescent Cspbx3 Nanocrystals: Water-Triggered Transformation through a Csx-Stripping Mechanism. *Nano Lett.* **2017**, *17*, 5799-5804.

(5) Hodges, J. M.; Schaak, R. E. Controlling Configurational Isomerism in Three-Component Colloidal Hybrid Nanoparticles. *Acc. Chem. Res.* **2017**, *50*, 1433-1440.

(6) Abeyweera, S. C.; Rasamani, K. D.; Sun, Y. Ternary Silver Halide Nanocrystals. *Acc. Chem. Res.* **2017**, *50*, 1754-1761.

(7) Sun, Y.; Zuo, X.; Sankaranarayanan, S.; Peng, S.; Narayanan, B.; Kamath, G. Quantitative 3d Evolution of Colloidal Nanoparticle Oxidation in Solution. *Science* **2017**, *356*, 303-307.

(8) Manna, L.; Scher, E. C.; Alivisatos, A. P. Synthesis of Soluble and Processable Rod-, Arrow-, Teardrop-, and Tetrapod-Shaped Cdse Nanocrystals. *J. Am. Chem. Soc.* **2000**, *122*, 12700-12706.

(9) Manna, L.; Milliron, D. J.; Meisel, A.; Scher, E. C.; Alivisatos, A. P. Controlled Growth of Tetrapod-Branched Inorganic Nanocrystals. *Nat. Mater.* **2003**, *2*, 382-385.

(10) Cheon, J.; Lee, J. H. Synergistically Integrated Nanoparticles as Multimodal Probes for Nanobiotechnology. *Acc. Chem. Res.* **2008**, *41*, 1630-1640.

(11) Yin, Y.; Alivisatos, A. P. Colloidal Nanocrystal Synthesis and the Organic-Inorganic Interface. *Nature* **2005**, *437*, 664-670.

(12) Chen, J.; Feng, J.; Yang, F.; Aleisa, R.; Zhang, Q.; Yin, Y. Space-Confined Seeded Growth of Cu Nanorods with Strong Surface Plasmon Resonance for Photothermal Actuation. *Angew. Chem. Int. Ed.* **2019**, *58*, 9275-9281.

(13) Gao, C.; Zhang, Q.; Lu, Z.; Yin, Y. Templated Synthesis of Metal Nanorods in Silica Nanotubes. *J. Am. Chem. Soc.* **2011**, *133*, 19706-19709.

(14) Cushing, B. L.; Kolesnichenko, V. L.; O'Connor, C. J. Recent Advances in the Liquid-Phase Syntheses of Inorganic Nanoparticles. *Chem. Rev.* **2004**, *104*, 3893-3946.

(15) Steimle, B. C.; Fenton, J. L.; Schaak, R. E. Rational Construction of a Scalable Heterostructured Nanorod Megalibrary. *Science* **2020**, *367*, 418-424.

(16) Moon, G.; Ko, S.; Min, Y.; Zeng, J.; Xia, Y.; Jeong, U. Chemical Transformations of Nanostructured Materials. *Nano Today* **2011**, *6*, 186-203.

(17) Kumar, A.; Jeon, K. W.; Kumari, N.; Lee, I. S. Spatially Confined Formation and Transformation of Nanocrystals within Nanometer-Sized Reaction Media. *Acc. Chem. Res.* **2018**, *51*, 2867-2879.

(18) Gao, A.; Xu, W.; Ponce de Leon, Y.; Bai, Y.; Gong, M.; Xie, K.; Park, B. H.; Yin, Y. Controllable Fabrication of Au Nanocups by Confined-Space Thermal Dewetting for Oct Imaging. *Adv. Mater.* **2017**, *29*, 1701070.

(19) Zhang, Q.; Ge, J.; Pham, T.; Goebl, J.; Hu, Y.; Lu, Z.; Yin, Y. Reconstruction of Silver Nanoplates by Uv Irradiation: Tailored Optical Properties and Enhanced Stability. *Angew. Chem. Int. Ed.* **2009**, *48*, 3516-3519.

(20) Sun, Y.; Wang, Y.; Chen, J.; Fujisawa, K.; Holder, C. F.; Miller, J. T.; Crespi, V. H.; Terrones, M.; Schaak, R. E. Interface-Mediated Noble Metal Deposition on Transition Metal Dichalcogenide Nanostructures. *Nat. Chem.* **2020**, *12*, 284-293.

(21) Smigelskas, A. D.; Kirkendall, E. O. Zinc Diffusion in Alpha Brass. *Trans. AIME* **1947**, *171*, 130-142.

(22) Gilroy, K. D.; Ruditskiy, A.; Peng, H. C.; Qin, D.; Xia, Y. Bimetallic Nanocrystals: Syntheses, Properties, and Applications. *Chem. Rev.* **2016**, *116*, 10414-10472.

(23) DeSantis, C. J.; Weiner, R. G.; Radmilovic, A.; Bower, M. M.; Skrabalak, S. E. Seeding Bimetallic Nanostructures as a New Class of Plasmonic Colloids. *J. Phys. Chem. Letters* **2013**, *4*, 3072-3082.

(24) Seitz, F. On the Porosity Observed in the Kirkendall Effect. *Acta Metallurgica* **1953**, *1*, 355-369.

(25) Li, X.; Wang, Z.; Zhang, Z.; Yang, G.; Jin, M.; Chen, Q.; Yin, Y. Construction of Au–Pd Alloy Shells for Enhanced Catalytic Performance toward Alkyne Semihydrogenation Reactions. *Mater. Horiz.* **2017**, *4*, 584-590.

(26) Chee, S. W.; Wong, Z. M.; Baraissov, Z.; Tan, S. F.; Tan, T. L.; Mirsaidov, U. Interface-Mediated Kirkendall Effect and Nanoscale Void Migration in Bimetallic Nanoparticles During Interdiffusion. *Nat. Commun.* **2019**, *10*, 2831.

(27) Li, X.; Wang, X.; Liu, M.; Liu, H.; Chen, Q.; Yin, Y.; Jin, M. Construction of Pd-M (M = Ni, Ag, Cu) Alloy Surfaces for Catalytic Applications. *Nano Res.* **2017**, *11*, 780-790.

(28) Hostetler, M.; Zhong, C.; Yen, B.; Anderegg, J.; Gross, S.; Evans, N.; Porter, M.; Murray, R. Stable, Monolayer-Protected Metal Alloy Clusters. *J. Am. Chem. Soc.* **1998**, *120*, 9396-9397.

(29) Link, S.; Wang, Z.; El-Sayed, M. A. Alloy Formation of Gold−Silver Nanoparticles and the Dependence of the Plasmon Absorption on Their Composition. *J. Phys. Chem. B* **1999**, *103*, 3529-3533.

(30) Shang, L.; Jin, L.; Guo, S.; Zhai, J.; Dong, S. A Facile and Controllable Strategy to Synthesize Au−Ag Alloy Nanoparticles within Polyelectrolyte Multilayer Nanoreactors Upon Thermal Reduction. *Langmuir* **2010**, *26*, 6713-6719.

(31) Mallin, M. P.; Murphy, C. J. Solution-Phase Synthesis of Sub-10 Nm Au−Ag Alloy Nanoparticles. *Nano Lett.* **2002**, *2*, 1235-1237.

(32) Russier-Antoine, I.; Bachelier, G.; Sablonière, V.; Duboisset, J.; Benichou, E.; Jonin, C.; Bertorelle, F.; Brevet, P. Surface Heterogeneity in Au-Ag Nanoparticles Probed by Hyper-Rayleigh Scattering. *Phys. Rev. B* **2008**, *78*.

(33) Wang, C.; Yin, H.; Chan, R.; Peng, S.; Dai, S.; Sun, S. One-Pot Synthesis of Oleylamine Coated Auag Alloy Nps and Their Catalysis for Co Oxidation. *Chem. Mater.* **2009**, *21*, 433-435.

(34) Pal, A.; Shah, S.; Devi, S. Preparation of Silver - Gold Alloy Nanoparticles at Higher Concentration Using Sodium Dodecyl Sulfate. *Aust. J. Chem.* **2008**, *61*.

(35) Rodriguez-Gonzalez, B. S.-I., A.; Giersig, M.; Liz-Marzan, L. M. Auag Bimetallic Nanoparticles: Formation, Silica-Coating and Selective Etching. *Faraday Discuss.* **2004**, *125*, 133-144.

(36) Liu, K.; Bai, Y.; Zhang, L.; Yang, Z.; Fan, Q.; Zheng, H.; Yin, Y.; Gao, C. Porous Au-Ag Nanospheres with High-Density and Highly Accessible Hotspots for Sers Analysis. *Nano Lett.* **2016**, *16*, 3675-3681.

(37) Bai, Y.; Gao, C.; Yin, Y. Fully Alloyed Ag/Au Nanorods with Tunable Surface Plasmon Resonance and High Chemical Stability. *Nanoscale* **2017**, *9*, 14875-14880.

(38) Xia, X.; Wang, Y.; Ruditskiy, A.; Xia, Y. 25th Anniversary Article: Galvanic Replacement: A Simple and Versatile Route to Hollow Nanostructures with Tunable and Well‐Controlled Properties. *Adv. Mater.* **2013**, *25*, 6313-6333.

(39) Yin, Y.; Erdonmez, C.; Aloni, S.; Alivisatos, A. P. Faceting of Nanocrystals During Chemical Transformation: From Solid Silver Spheres to Hollow Gold Octahedra. *J. Am. Chem. Soc.* **2006**, *128*, 12671-12673.

(40) Kubaschewski, O. The Diffusion Rates of Some Metals in Copper, Silver, and Gold. *Trans. Faraday Soc.* **1950**, *46*, 713-722.

(41) Gonzalez, E.; Arbiol, J.; Puntes, V. F. Carving at the Nanoscale: Sequential Galvanic Exchange and Kirkendall Growth at Room Temperature. *Science* **2011**, *334*, 1377-1380.

(42) Chee, S. W.; Tan, S. F.; Baraissov, Z.; Bosman, M.; Mirsaidov, U. Direct Observation of the Nanoscale Kirkendall Effect During Galvanic Replacement Reactions. *Nat. Commun.* **2017**, *8*, 1224.

(43) Yin, Y.; Erdonmez, C. K.; Cabot, A.; Hughes, S.; Alivisatos, A. P. Colloidal Synthesis of Hollow Cobalt Sulfide Nanocrystals. *Adv. Funct. Mater.* **2006**, *16*, 1389-1399.

(44) Chen, M.; Hu, H.; Tan, Y.; Yao, N.; Zhong, Q.; Sun, B.; Cao, M.; Zhang, Q.; Yin, Y. Controlled Growth of Dodecapod-Branched Cspbbr3 Nanocrystals and Their Application in White Light Emitting Diodes. *Nano Energy* **2018**, *53*, 559-566.

(45) Zhang, Q.; Yin, Y. All-Inorganic Metal Halide Perovskite Nanocrystals: Opportunities and Challenges. *ACS Cent. Sci.* **2018**, *4*, 668-679.

(46) Zhong, Q.; Cao, M.; Hu, H.; Yang, D.; Chen, M.; Li, P.; Wu, L.; Zhang, Q. One-Pot Synthesis of Highly Stable Cspbbr3@Sio2 Core-Shell Nanoparticles. *ACS Nano* **2018**, *12*, 8579-8587.

(47) Hu, H.; Wu, L.; Tan, Y.; Zhong, Q.; Chen, M.; Qiu, Y.; Yang, D.; Sun, B.; Zhang, Q.; Yin, Y. Interfacial Synthesis of Highly Stable Cspbx3/Oxide Janus Nanoparticles. *J. Am. Chem. Soc.* **2018**, *140*, 406-412.

(48) Wang, D.; Wang, X.; Li, Z.; Chi, M.; Li, Y.; Liu, Y.; Yin, Y. Migration of Iron Oxide Nanoparticle through a Silica Shell by the Redox-Buffering Effect. *ACS Nano* **2018**, *12*, 10949-10956.

(49) Feng, J.; Yin, Y. Self-Templating Approaches to Hollow Nanostructures. *Adv. Mater.* **2019**, *31*, 1802349.

(50) Hu, Y.; Ge, J.; Sun, Y.; Zhang, T.; Yin, Y. A Self-Templated Approach to Tio2 Microcapsules. *Nano Lett.* **2007**, *7*, 1832-1836.

(51) Zhang, Q.; Zhang, T.; Ge, J.; Yin, Y. Permeable Silica Shell through Surface-Protected Etching. *Nano Lett.* **2008**, *8*, 2867-2871.

(52) Zhang, Q.; Ge, J.; Pham, T.; Goebl, J.; Hu, Y.; Lu, Z.; Yin, Y. Rattle-Type Silica Colloidal Particles Prepared by a Surface-Protected Etching Process. *Nano Res.* **2010**, *2*, 583-591.

(53) Xu, W.; Wang, M.; Li, Z.; Wang, X.; Wang, Y.; Xing, M.; Yin, Y. Chemical Transformation of Colloidal Nanostructures with Morphological Preservation by Surface-Protection with Capping Ligands. *Nano Lett.* **2017**, *17*, 2713-2718.

(54) Xu, W.; Lyu, F.; Bai, Y.; Gao, A.; Feng, J.; Cai, Z.; Yin, Y. Porous Cobalt Oxide Nanoplates Enriched with Oxygen Vacancies for Oxygen Evolution Reaction. *Nano Energy* **2018**, *43*, 110-116.

(55) Lyu, F.; Bai, Y.; Wang, Q.; Wang, L.; Zhang, X.; Yin, Y. Coordination-Assisted Synthesis of Iron-Incorporated Cobalt Oxide Nanoplates for Enhanced Oxygen Evolution. *Mater. Today Chem.* **2019**, *11*, 112-118.

(56) Li, B.; Chen, J.; Han, L.; Bai, Y.; Fan, Q.; Wu, C.; Wang, X.; Lee, M.; Xin, H.; Han, Z.; Yin, Y. Ligand-Assisted Solid-State Transformation of Nanoparticles. *Chem. Mater.* **2020**, *32*, 3271-3277.

(57) Lavine, M. S. A Hot Way to Change Shape. *Science* **2020**, *368*, 150.